Proc. Natl. Acad. Sci. USA
Vol. 96, pp. 8259–8264, July 1999
Physiology

Intracellular Ca^{2+} oscillations drive spontaneous contractions in cardiomyocytes during early development

S. VIATCHENKO-KARPINSKI*, B. K. FLEISCHMANN*, Q. LIU, H. SAUER, O. GRYSHCHENKO, G. J. JI, AND J. HESCHELER†

Institute of Neurophysiology, University of Cologne, Robert-Koch-Strasse 39, 50931 Köln, Germany

Communicated by Robert E. Forster, University of Pennsylvania School of Medicine, Philadelphia, PA, April 19, 1999 (received for review December 21, 1998)

ABSTRACT **Activity of cardiac pacemaker cells is caused by a balanced interplay of ion channels. However, it is not known how the rhythmic beating is initiated during early stages of cardiomyogenesis, when the expression of ion channels is still incomplete. Based on the observation that early-stage embryonic stem cell-derived cardiomyocytes continuously contracted in high extracellular K^+ solution, here we provide experimental evidence that the spontaneous activity of these cells is not generated by transmembrane ion currents, but by intracellular $[Ca^{2+}]_i$ oscillations. This early activity was clearly independent of voltage dependent L-type Ca^{2+} channels and the interplay between these and ryanodine sensitive Ca^{2+} stores. We also show that intracellular Ca^{2+} oscillations evoke small membrane depolarizations and that these can trigger L-type Ca^{2+} channel driven action potentials.**

It is postulated that the heart is contracting because of the electromechanical coupling. First, an action potential (AP) is evoked leading to the opening of voltage-dependent L-type Ca^{2+} channels (VDCCs). Second, the Ca^{2+} entering into the cardiomyocyte through VDCC triggers the release of Ca^{2+} from the ryanodine-sensitive Ca^{2+} stores [Ca^{2+}-induced Ca^{2+} release (CICR)], leading to a marked increase of the free cytosolic Ca^{2+} concentration ($[Ca^{2+}]_i$) (1–4). This mechanism raises $[Ca^{2+}]_i$ high enough to initiate the interaction of the contractile filaments and subsequent contractions. Additional confirmation of this hypothesis has been provided by the finding of Ca^{2+} sparks (5).

In the sinus node and the cells of the conduction system, VDCCs are rhythmically activated by diastolic depolarizations and related APs (6–9). The hyperpolarization activated non-selective cation current (I_f) underlying these spontaneous diastolic depolarizations (10) has recently been cloned (11–13).

The rhythmic APs, CICR, and contractions require the functional expression of a variety of membrane ion channels and intracellular Ca^{2+} release sites (14), as well as Ca^{2+} extrusion mechanisms (15). Previous studies showed, however, that murine embryonic cardiomyocytes do not express the full ensemble of ion channels and that some channels are expressed at lower densities (16, 17, 17, 18). Therefore, we wondered whether these cells displayed already spontaneous electrical activity and CICR.

Cardiomyocytes before day embryonic day 11 post coitum, cannot be obtained from the embryo because the heart is too small to be subjected to single cell preparations (17). Recent work has established the embryoid body (EB) cell system as a tool for the investigation of early cardiomyogenesis (18–20). Ultrastructural (18), molecular biological (21), and electrophysiological (16, 22) studies have demonstrated that, within the EB, the various stages of cardiomyogenesis parallel the murine heart development.

Here, we provide evidence that spontaneous contractions of early cardiomyocytes differentiated within EBs do not require CICR but are triggered by $[Ca^{2+}]_i$ oscillations. We further show that these $[Ca^{2+}]_i$ oscillations, rather than CICR, induce the earliest APs in these cardiomyocytes.

MATERIALS AND METHODS

Cell Preparation. Cardiomyocytes were derived from the pluripotent embryonic stem (ES) cell line D3 (19, 20). The differentiation protocol was similar, as described before (16, 20). In brief, undifferentiated ES cells were cultivated on feeder layers and, for passaging, were dispersed with trypsin. Embryoid bodies (EBs) were generated by cultivating the ES cells first for 2 days in hanging drops (400 cells/20 μl), then for 5 days in suspension, and finally by plating for 1–15 days on gelatin-coated glass coverslips. About 12–24 hours after plating, spontaneously contracting cell clusters appeared. For the preparation of isolated stage-1 (differentiated for 9 days), stage-2 (differentiated for 10–11 days), and stage-4 (differentiated for 17–22 days) cardiomyocytes, beating areas of 20–30 EBs were dissected and isolated by enzymatic dispersion by using collagenase B (Boehringer Ingelheim), as described in more detail by Maltsev *et al.* (16). The solution used for dissociation of the dissected areas contained (in mM): NaCl 120, KCl 5.4, $MgSO_4$ 5, $CaCl_2$ 0.03, Na pyruvate 5, glucose 20, taurine 20, Hepes 10, collagenase B 0.5–1 mg/ml, pH 6.9 (NaOH). The dissociated material was plated onto glass coverslips and was stored in the incubator. Within the first 12 hours, cells attached to the glass surface.

Electrophysiology. For electrophysiological recordings, the glass coverslips were transferred to a temperature-controlled recording chamber and were superfused with extracellular solution. Only spontaneously beating cells were selected for the experiments. Cellular electrical activity was recorded in the current-clamp and voltage-clamp mode (23) by using the perforated patch-clamp configuration (24). Ionic currents were recorded by using an Axopatch 200 A (Axon Instruments, Foster City, CA) or an EPC-9 amplifier (HEKA Electronics, Lambrecht/Pfalz, Germany). Data were acquired by using the ISO 2 (MFK, Niedernhausen, Germany) or the PULSE (HEKA Electronics) software package. Data were digitized at 10 kHz and were filtered at 1 kHz.

Pipettes (3–4 megaohms) were prepared on a DMZ Universal Puller (DMZ, München, Germany) from 1.5-mm bo-

The publication costs of this article were defrayed in part by page charge payment. This article must therefore be hereby marked "*advertisement*" in accordance with 18 U.S.C. §1734 solely to indicate this fact.

PNAS is available online at www.pnas.org.

Abbreviations: AP, action potential; VDCC, voltage-dependent L-type Ca^{2+} channels; CICR, Ca^{2+}-induced Ca^{2+} release; EB, embryonic body; ES cell, embryonic stem cell; CLSM, confocal laser scanning microscopy.

*S.V.-K. and B.K.F. contributed equally to the manuscript.
†To whom reprint requests should be addressed. e-mail: JH@physiologie.uni-koeln.de.

rosilicate glass capillaries (Clark Electromedical Instruments, Reading, U.K.). The composition of the different recording solutions used was the following (in mM): Extracellular solutions: NaCl 140, KCl 5, $CaCl_2$ 2, $MgCl_2$ 2, Hepes 5, and glucose 10; high K^+ solution: NaCl 5, KCl 140, $CaCl_2$ 2, $MgCl_2$ 2, Hepes 5, and glucose 10; low Na^+ solution: NaCl 15, KCl 5, CholineCl 120, $CaCl_2$ 2, $MgCl_2$ 2, Hepes 5, and glucose 10; low Na^+-, high K^+ solution: NaCl 15, KCl 140, $MgCl_2$ 2, Hepes 5, and glucose 10, pH 7.4 (NaOH); intracellular solution: KCl 55, K_2SO_4 70, $MgCl_2$ 7, and Hepes 10, pH 7.4 (KOH). Amphotericin B (Sigma) was dissolved (7.5 mg) as stock solution in 125 μl of DMSO. The pipette was backfilled with amphotericin containing intracellular solution, and the pipette tip was shortly put into amphotericin free intracellular solution. The final concentration of amphotericin B in the pipette solution was 1 mg/ml. The series resistance reached a steady-state level of 10–20 megaohms within 5–15 min after obtaining a gigaohm seal. All experiments were carried out at 35–37°C. Data are given as means ± SEM.

$[Ca^{2+}]_i$ Measurements with the Photomultiplier Tube. Cells were loaded for 12–15 min in DMEM with the cell-permeable dye fura-2AM (1 μM, Molecular Probes) at 37°C. Then, coverslips were transferred to a temperature-controlled recording chamber and were perfused for 10 min with extracellular solution before the start of the experiments. Superfusion was performed by gravity at a rate of 1 ml/min. A 90% volume exchange was achieved within ≈10 sec. Monochromic excitation light (340, 380 nm) was generated by a monochromator at a frequency of 50 Hz (TILL Photonics, Planegg, Germany). The monochromator was coupled to the epifluorescence attachment of an inverted microscope (Zeiss, 135M) through a small quartz light guide. The excitation light was directed to the objective (40×, Zeiss) via a dichroic mirror (TILL Photonics). The emitted fluorescence from the fura-2 loaded cells was monitored through a 470-nm interference filter by using a photomultiplier attached to the anterior port of the microscope. Spontaneously beating cardiomyocytes were investigated. The cell of interest was identified before the experiment, and other cells were excluded from the visual field with an iris mounted on the epifluorescence attachment. Fluorescence intensities were stored on a videotape by using a pulse-code modulator (VR 100, Instrutech, Mineola, NY). Background fluorescence was determined at the end of the experiments by removing the cell of interest from the visual field and determining the remaining fluorescence. The fluorescence of unloaded cardiomyocytes was negligible. For analysis, data were downloaded from the videotape via pulse-code modulator into an Axon software program (Axon Instruments) at a sampling rate of 250 Hz and were filtered at 100 Hz. Files in ASCII format were imported into a spreadsheet program (SIGMA PLOT, Jandel Scientific, Erkrath, Germany), and background intensities were subtracted at both wavelengths individually. The data are displayed as 340/380 ratios.

Confocal Laser Scanning Microscopy (CLSM). $[Ca^{2+}]_i$ was monitored in whole EBs as well as in single cardiac cells by using the fluorescent dye fluo-3, AM (Molecular Probes). Cells were loaded for 15 min in DMEM with 10 μM fluo-3, AM and were dissolved in dimethyl sulfoxide (final concentration 0.1%) and pluronic F-127 (Molecular Probes, final concentration <0.025%). Then, the coverslips were rinsed in the standard extracellular solution and were transferred to the recording chamber. Fluo-3 fluorescence was monitored by an inverted CLSM (LSM 410, Zeiss) using a 25× objective numerical aperture 0.80 (Neofluar, Zeiss). For fluorescence excitation, the 488-nm band of an argon laser was used. Emission was recorded by using a longpass LP 515 filter set. Pixel images (265 × 265 and 128 × 100 images) were acquired every 0.36 and 0.15 sec, respectively. To determine contractions of cardiomyocytes, transmission images and fluorescence images were recorded simultaneously by using the overlay option of the confocal setup. Contractions of cardiomyocytes caused changes in light diffraction in the transmission image and were monitored as deviations from the basal gray level. Processing of images was carried out by using the time-software facilities of the confocal setup. Images were acquired and stored to 16-megabyte video memory of the confocal setup at the selected time intervals indicated. Each series of images was scaled between pixel intensity 0 (background fluorescence) and 255 (maximum fluorescence in that series). The pixel values in a region of interest (selected by using an overlay mask) were analyzed by using SIGMA PLOT. The fluorescence changes occurring within single cells during the time course of the experiment were individually recorded, and the data were presented in arbitrary units as percentage of fluorescence variation F with respect to the resting level F_0.

Test Substances. Bay K 8644 and nisoldipine (kindly provided by Bayer AG, Leverkusen, Germany) were dissolved in ethanol (final concentration <0.1%) and thapsigargin (Molecular Probes) was dissolved in DMSO (final concentration <0.1%). All remaining substances used were purchased from Sigma, were dissolved to the final concentration in extracellular solution, and were applied by gravitational flow. Caffeine was applied through a puffer pipette (General Valve, Fairfield, NJ).

RESULTS

Pluripotent, murine ES cells of the cell line D3 were differentiated as EBs to investigate stage-1 (differentiated for 8–9 days) and stage-2 (differentiated for 10–11 days) cardiomyocytes corresponding to a stage before embryonic day 11 post coitum of the murine embryonic heart. Terminally differentiated (stage 4) cardiomyocytes (differentiated for 16–22 days) resembled the different cardiac cell phenotypes of murine neonates (16, 19, 20).

Our study was initiated by the observation that stage-1 and -2 cardiomyocytes stably contracted for hours under conditions in which the membrane potential was depolarized by superfusion with 140 mM K^+. A similar contraction frequency of ≈1 Hz occurred in the presence of physiological saline solution and high K^+. This feature was not observed in stage-4 ES cell-derived cardiomyocytes, which, similarly to adult cardiomyocytes, showed hypercontraction and cell death within seconds of exposure to high K^+.

Because omission of extracellular Ca^{2+} did not stop contractions immediately, we examined whether rhythmic changes of $[Ca^{2+}]_i$ generated these contractions in stage-1 and -2 cardiomyocytes. By using CLSM as well as photometry, $[Ca^{2+}]_i$ was measured under physiological conditions, in the presence of 140 mM K^+, and after pharmacological intervention. As seen in Fig. 1*A*, $[Ca^{2+}]_i$ oscillations were observed with the cells in normal extracellular solution. Application of high K^+ led to a transient rise of $[Ca^{2+}]_i$, presumably because of the activation of VDCC. During the declining phase rhythmic, large-amplitude $[Ca^{2+}]_i$ oscillations occurred. These were time-locked with the spontaneous contractile activity ($n = 3$), indicating that they were driven by the $[Ca^{2+}]_i$ oscillations. Spontaneously contracting fura-2 loaded stage-1 and -2 cardiomyocytes displayed deflections of 340/380-nm signals in opposite directions. This excluded that the observed changes of $[Ca^{2+}]_i$ were evoked by movement artifacts. To further confirm that $[Ca^{2+}]_i$ oscillations are unrelated to membrane channels, different pharmacological agents were tested in regard to their efficacy in interrupting the oscillations (Fig. 1 *B–D*). The persistence of $[Ca^{2+}]_i$ oscillations and contractions under high K^+ made the involvement of VDCC unlikely. This was corroborated by the observation that $[Ca^{2+}]_i$ oscillations continued in the presence of the selective VDCC blocker nisoldipine (2 μM) (Fig. 1*B*, $n = 5$). The significantly faster decline of the 340/380 ratio in normal extracellular solution as

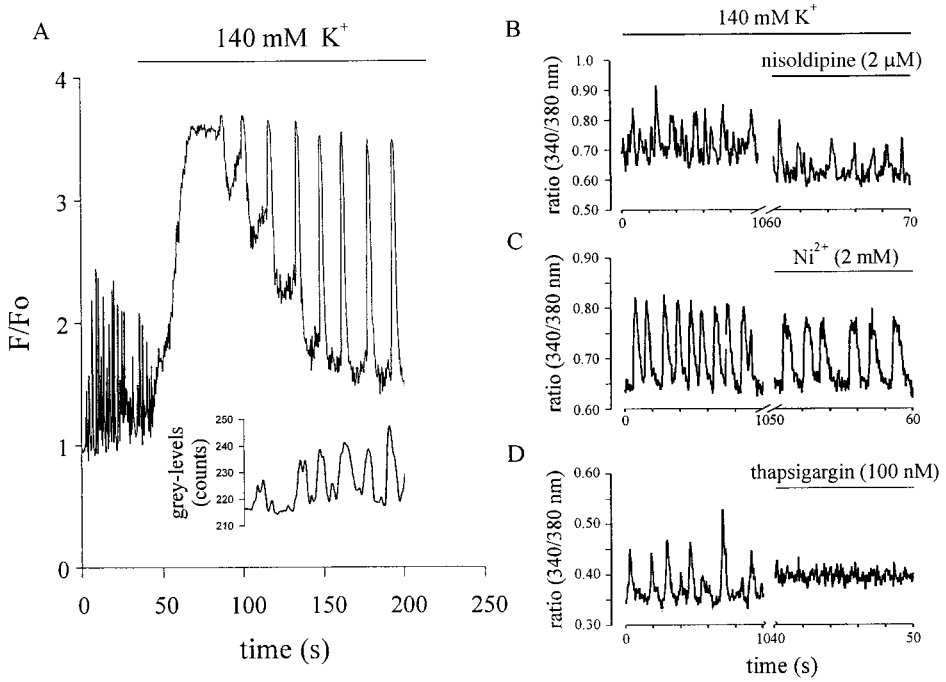

FIG. 1. (*A*) Effect of high K^+ on $[Ca^{2+}]_i$ oscillations and contractions observed with CLSM in a single stage-2 cardiomyocyte. Depolarization resulted in a transient rise of $[Ca^{2+}]_i$, presumably because of the activation of VDCC channels and in an alteration of the amplitude and frequency of oscillations. The inset shows cell contractions time-locked with $[Ca^{2+}]_i$ oscillations during superfusion with high K^+. Cell membrane depolarization resulted in an initial discontinuation of contractions, which resumed with the decline of $[Ca^{2+}]_i$. F/Fo indicates the ratio between the actual and the initial intensity of the fluorescent dye. Grey-levels represent the intensity of the transmitted light, which varied with cell contraction. (*B–D*) Effect of different pharmacological agents on 340/380 ratios in fura-2AM-loaded spontaneously beating stage-2 cells. (*B*) The VDCC blocker nisoldipine (2 μM) did not impair $[Ca^{2+}]_i$ oscillations but lead to a lowering of steady-state $[Ca^{2+}]_i$ levels. (*C*) Similarly, Ni^{2+} (2 mM), known to block the Na^+-Ca^{2+} exchanger, did not interrupt $[Ca^{2+}]_i$ oscillations. (*D*) The Ca^{2+}-ATPase inhibitor thapsigargin (100 nM) led to an abrupt halt of the $[Ca^{2+}]_i$ oscillations and a concomitant increase of the resting $[Ca^{2+}]_i$.

compared with high K^+ solution indicated the functional expression of the Na^+-Ca^{2+} exchanger in stage-1 and -2 cardiomyocytes (n = 11) (25, 26). However, it is unlikely that the Na^+-Ca^{2+} exchanger evoked the $[Ca^{2+}]_i$ oscillations through its backward mode (27) or its reduced activity in high K^+ (28) because these persisted even after addition of 2 mM Ni^{2+}, a known blocker of the Na^+-Ca^{2+} exchanger (Fig. 1*C*; note the slowing of the decline of the 340/380 ration, n = 2) or Ni^{2+} plus nisoldipine (n = 3, data not shown). In contrast, thapsigargin, a sarcoplasmic Ca^{2+}-ATPase inhibitor, led to a rise in $[Ca^{2+}]_i$ and an abrupt halt of $[Ca^{2+}]_i$ oscillations (Fig. 1*D*, n = 7), showing that these intracellular $[Ca^{2+}]_i$ oscillations drive spontaneous contractions in stage-1 and -2 cardiomyocytes.

To examine whether the $[Ca^{2+}]_i$ oscillations translated into changes of the membrane potential, current clamp experiments were performed. Stage-1 cells were characterized by a depolarized resting potential (minimal diastolic potential, -56 ± 14 mV, n = 14) and APs of small amplitude ($\leq$30 mV, Fig. 2*A*). Most of the stage-2 cells also showed depolarized resting potentials (-62 ± 10 mV, n = 9) but already displayed APs of larger amplitude ($\geq$30 mV, Fig. 2 *B* and *C*). Stage-1 and most of the stage-2 cardiomyoctes were characterized by small fluctuations of the membrane potential intercalated between the APs (Fig. 2 *A–C*). These fluctuations occurred at a frequency of 1.3 ± 0.5 Hz (n = 18), were associated with spontaneous contractions of the cells, and proved to depend on the resting potential. In cardiomyocytes with resting potentials negative to -40 mV, the average amplitude amounted to 17 ± 1 mV (n = 19), and, in those with resting potentials positive to -40 mV, the amplitude was 9 ± 2 mV (n = 8). Stage-4 sinusnodal-like cardiomyocytes displayed diastolic depolarizations (Fig. 2*D*). These cells are known to express I_f and $I_{K,\,ACh}$ (16). In contrast to stage 1 and 2, stage-4 cardiomyocytes did not display the small fluctuations (see Fig. 2*D*), suggesting a correlation between the $[Ca^{2+}]_i$ oscillations and the membrane potential fluctuations. Therefore, the origin of these was further investigated by pharmacological tools. Superfusion with 140 mM K^+ depolarized the resting potential of stage-1 and -2 cells close to 0 mV and interrupted both APs and membrane potential fluctuations (Fig. 3*A*, n = 4). However, the cardiomyocytes continued to display spontaneous contractions (microscopic observation). Addition of the VDCC blocker nisoldipine (50 nM, n = 4) interrupted the generation of APs but not the membrane potential fluctuations and the accompanying contractions (Fig. 3*B*). APs and membrane potential fluctuations as well as contractions were completely blocked by addition of thapsigargin (Fig. 3*C*, 100 nM, n = 3). These data indicate that (*i*) the membrane potential fluctuations do not trigger the $[Ca^{2+}]_i$ oscillations, (*ii*) the fluctuations depend on the filling state of intracellular Ca^{2+} stores, (*iii*) the fluctuations are independent of the opening of VDCC, and (*iv*) the APs are triggered by the fluctuations. Hence, Ca^{2+} imaging and patch-clamp experiments in the current clamp mode demonstrate that spontaneous contractions of cardiomyocytes during early development depend neither on the membrane potential nor on the transmembrane L-type Ca^{2+} current but are governed by $[Ca^{2+}]_i$ oscillations.

Because early APs are not required for the generation of contractions, they must serve another function in the early embryonic heart. It is known that ES cell-derived cardiomyocytes express connexin, forming functional gap-junctions very early during development (29). Hence, we wondered whether the early APs are required to provide synchronization of contractions between cardiomyocytes. Therefore, isolated clusters of cardiomyocytes were loaded with the cell permeable dye fluo3-AM. CLSM revealed Ca^{2+} waves propagating with a velocity of 300 ± 64 μm/sec (n = 3). Waves synchronous with

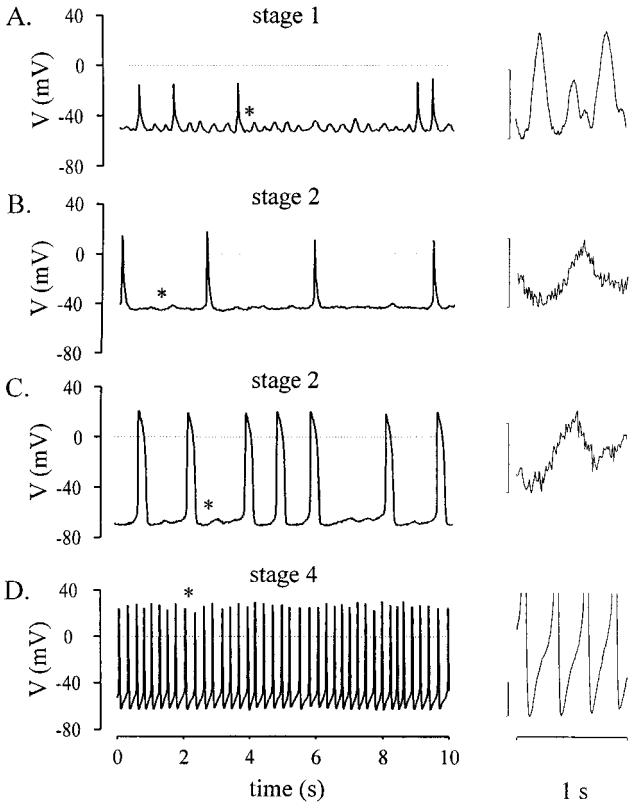

FIG. 2. Electrical activity recorded in spontaneously beating ES cell-derived cardiomyocytes in the current clamp mode. (*A*) Typical recording from a stage-1 cell with depolarized resting potential and APs of small amplitude. Membrane potential fluctuations (marked by an asterisk) shown at extended scales (vertical calibration bar represents 10 mV) on the right were intercalated between APs. (*B*) Stage-2 cells displayed typically depolarized resting potentials but larger APs than stage-1 cells. The membrane potential fluctuations were still observed. (*C*) Transitional stage (stage 2) cell, which displayed a more negative resting potential and small diastolic depolarizations before the generation of APs. Membrane potential fluctuations were still present. (*D*) Stage-4 pacemaker-like cells were characterized by an unstable resting potential and the typical diastolic depolarization.

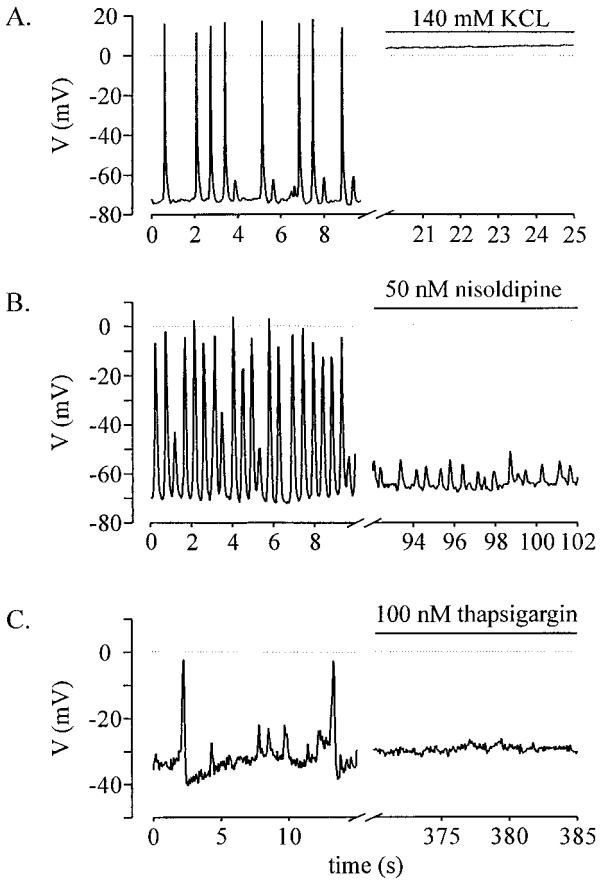

FIG. 3. Pharmacological characterization of the APs and membrane potential fluctuations in spontaneously beating stage-1 and -2 cells measured under current clamp. (*A*) Superfusion of 140 mM K^+ led to depolarization of the resting potential close to 0 mV and halted both APs and small membrane potential fluctuations. (*B*) Superfusion of the VDCC blocker nisoldipine (50 nM) interrupted the APs but not the small membrane potential fluctuations. (*C*) Application of the sarcoplasmic ATPase inhibitor thapsigargin (100 nM) to a stage-1 cell blocked both APs and membrane potential fluctuations and led to a depolarization of the resting potential.

cell contractions were observed in single cells as well as in beating foci in plated EBs, excluding Ca^{2+} overload caused by cell damage by enzymatic dissociation as the underlying mechanism. Fig. 4 shows recordings of $[Ca^{2+}]_i$ in normal extracellular solution (Fig. 4*A*) as well as on superfusion with high K^+-solution (Fig. 4*B*). Under control conditions, the Ca^{2+} wave spread in a coordinated manner, indicating an electrical coupling between the cardiomyocytes through gap junctions. The initiation site and the direction of propagation of the waves remained unaltered during the course of the experiment. In high K^+-solution, the $[Ca^{2+}]_i$ oscillations persisted but occurred in a desynchronized manner. No initiation site or direction of propagation could be identified. Further, the frequency and amplitude of the $[Ca^{2+}]_i$ oscillations differed markedly between individual cells (Fig. 4*B*).

DISCUSSION

The heart is the first organ to form during embryonic development. The autonomic rhythm can be observed as early as in embryonic day 9.5 of murine embryonic development (30). The major finding of our study is that contractions of the heart during early development are not evoked by transmembrane ion currents resulting in APs but by intracellular $[Ca^{2+}]_i$ oscillations. Further, CICR is not required for functioning of the early embryonic heart because ES cell-derived stage-1 and -2 cardiomyocytes continued to contract under high K^+ when the membrane potential was depolarized. These findings differ from those suggesting that electromechanical coupling in the fetal heart depends largely on trans-sarcolemmal Ca^{2+} influx rather than Ca^{2+} released from the sarcoplasmic reticulum (31–34). However, these studies were performed at late embryonic stages whereas the work presented here investigates early embryonic cardiomyocytes. Membrane potential-independent contractions are in complete contrast to the functioning of the adult heart, where incubation of heart tissue in high extracellular K^+ solution (cardioplegic solution) is used as standard procedure to prevent contractions.

Thus, the present findings envision intracellular Ca^{2+} stores as the primary rhythm generator in murine cardiomyocytes early during development whereas VDCC may serve primarily for store refilling (35). The increase of $[Ca^{2+}]_i$ leads to activation of a Ca^{2+}-activated conductance (nonselective cation current and/or Na^+-Ca^{2+} exchanger), resulting in the small depolarization of the resting potential and the occasional generation of APs via activation of VDCC, similar to observations made on cultured cardiac cells (36). Preliminary experimental results on the nature of this Ca^{2+} activated conductance under a $[Ca^{2+}]_i$ increase induced by caffeine point toward a nonselective cation current because the reversal potential of this current was close to 0 mV and shifted to more negative potentials on replacement of extracellular Na^+ by

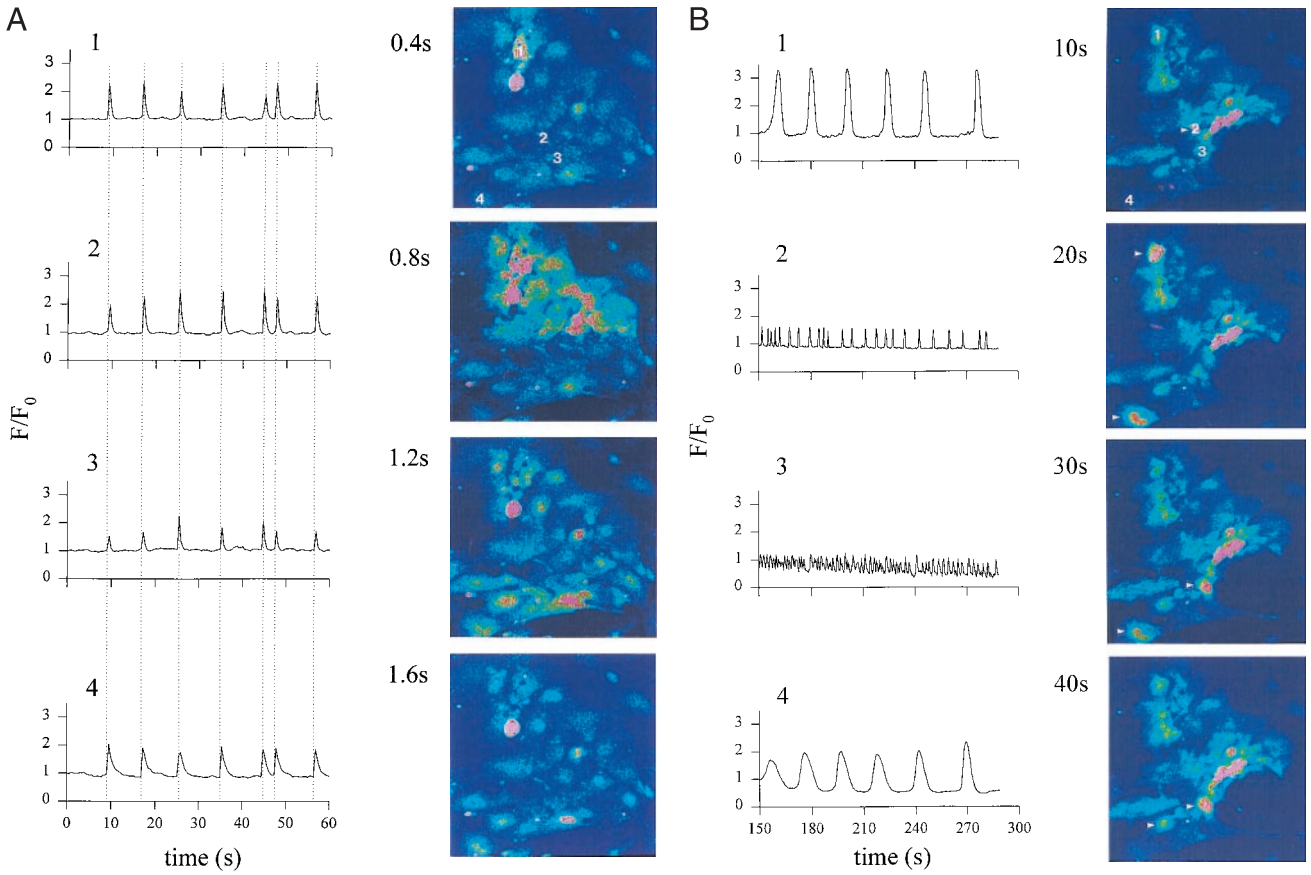

FIG. 4. CLSM images of $[Ca^{2+}]_i$ oscillations in a spontaneously contracting area of cardiomyocytes isolated from a stage-2 EB. (*A*) Control conditions. A $[Ca^{2+}]_i$ wave spread with a velocity of $\approx$400 μm·sec^{-1} from the initiation site (cell 1) to the termination site (cell 4). The tracings of $[Ca^{2+}]_i$ changes in different cells (cell 1–4) demonstrate the synchronization of the $[Ca^{2+}]_i$ signal, indicating electrical coupling between adjacent cells. (*B*) $[Ca^{2+}]_i$ oscillations recorded in the same area of cardiomyocytes after superfusion with high K^+. The images were recorded after decline toward resting $[Ca^{2+}]_i$ of the initial transient $[Ca^{2+}]_i$ rise after switching to high K^+. The initial $[Ca^{2+}]_i$ increase was caused by the activation of VDCC. Note that, under high K^+ $[Ca^{2+}]_i$, oscillations in cells 1–4 are desynchronized and differ in amplitude and frequency.

choline. This behavior is clearly different from the characteristics of the Na^+-Ca^{2+} exchanger-mediated current (25, 26, 37, 38). In contrast to early-stage cardiomyocytes, terminally differentiated pacemaker cells were characterized by membrane driven events. In these cells, interplay between different ion channels, in particular VDCC, K^+ channels, and I_f, allows the generation of spontaneous activity, governing the heart beat (6, 8, 9, 39).

Because we clearly demonstrated that APs do not translate into CICR, we investigated whether they serve to synchronize the heart beat. In multicellular preparations, the cardiomyocytes were electrically coupled by gap junctions, even at this early developmental stage (29). The pacemaker cell with the highest frequency of $[Ca^{2+}]_i$ oscillations (internal oscillator) determined the contractile activity of the whole cardiomyocyte cluster. Application of high extracellular K^+ caused the cardiomyocytes to electrically uncouple and contract again under control of their internal oscillator (40). It is tempting to speculate that this very early motif is even found in cardiomyocytes before the onset of spontaneous APs. Indeed, an oscillatory behavior of the resting potential at this very early stage was observed by using membrane potential-sensitive dyes in combination with photodiode arrays (41). Subsequently, APs coupled with contractions were observed in the embryonic rat heart at embryonic day 9.5 (42).

There is evidence that mechanisms important during early embryonic development may remain dormant in terminally differentiated cells but may assume *de novo* significance in the case of pathological cell transformation. It can be speculated that, in certain pathological conditions, the internal oscillator (40) again becomes predominant and induces cardiac arrhythmias, as suggested for ouabain intoxication or extended β-adrenergic stimulation. The resemblance between embryonic and pathologically transformed cells may be related to the functional expression of Ca^{2+} activated conductances (36, 43–45). Thus, Ca^{2+} overload associated with spontaneous Ca^{2+} release from intracellular Ca^{2+} stores (46, 47) may result in the generation of arrhythmias: i.e., delayed after depolarizations (44, 48).

We thank Dr. A. M. Wobus for providing ES cells of the cell line D3, M. Faulhaber and B. Hops for assistance in cell culture work, Dr. M. Morad (Georgetown University), Dr. Ganitkevich, and Dr. S. Herzig (University of Cologne) for reading an earlier version of the manuscript and helpful discussions. We further thank Dr. N. Smyth (University of Cologne) for critically reading the final version of the manuscript. The support of the machine and electronic shop is greatly acknowledged.

1. Fabiato, A. (1985) *J. Gen. Physiol.* **85,** 247–289.
2. du Bell, W. H. & Houser, S. R. (1987) *Cell Calcium* **8,** 259–268.
3. Barcenas-Ruiz, L. & Wier, W. G. (1987) *Circ. Res.* **61,** 148–154.
4. Nabauer, M., Callewaert, G., Cleemann, L. & Morad, M. (1989) *Science* **244,** 800–803.
5. Cheng, H., Lederer, W. J. & Cannell, M. B. (1993) *Science* **262,** 740–744.
6. Noble, D. (1983) *Symp. Soc. Exp. Biol.* **37,** 1–28.
7. Brown, H. F., Kimura, J., Noble, D., Noble, S. J. & Taupignon, A. (1984) *Proc. R. Soc. London Ser. B* **222,** 329–347.
8. Denyer, J. C. & Brown, H. F. (1990) *J. Physiol. (London)* **428,** 405–424.

9. Irisawa, H., Brown, H. F. & Giles, W. (1993) *Physiol. Rev.* **73,** 197–227.
10. DiFrancesco, D. (1993) *Annu. Rev. Physiol.* **55,** 455–472.
11. Ludwig, A., Zong, X., Jeglitsch, M., Hofmann, F. & Biel, M. (1998) *Nature (London)* **393,** 587–591.
12. Gauss, R., Seifert, R. & Kaupp, U. B. (1998) *Nature (London)* **393,** 583–587.
13. Santoro, B., Liu, D. T., Yao, H., Bartsch, D., Kandel, E. R., Siegelbaum, S. A. & Tibbs, G. R. (1998) *Cell* **93,** 717–729.
14. Bers, D. M. (1997) *Circ. Res.* **81,** 636–638.
15. Bers, D. M. (1997) *Basic Res. Cardiol.* **92,** Suppl. 1, 1–10.
16. Maltsev, V. A., Wobus, A. M., Rohwedel, J., Bader, M. & Hescheler, J. (1994) *Circ. Res.* **75,** 233–244.
17. Davies, M. P., An, R. H., Doevendans, P., Kubalak, S., Chien, K. R. & Kass, R. S. (1996) *Circ. Res.* **78,** 15–25.
18. Hescheler, J., Fleischmann, B. K., Lentini, S., Maltsev, V. A., Rohwedel, J., Wobus, A. M. & Addicks, K. (1997) *Cardiovasc. Res.* **36,** 149–162.
19. Doetschman, T. C., Eistetter, H., Katz, M., Schmidt, W. & Kemler, R. (1985) *J. Embryol. Exp. Morphol.* **87,** 27–45.
20. Wobus, A. M., Wallukat, G. & Hescheler, J. (1991) *Differentiation (Berlin)* **48,** 173–182.
21. Miller-Hance, W. C., La Corbiere, M., Fuller, S. J., Evans, S. M., Lyons, G., Schmidt, C., Robbins, J. & Chien, K. R. (1993) *J. Biol. Chem.* **268,** 25244–25252.
22. Ji G. J., Fleischmann B. K., Bloch, W., Feelisch, M., Andressen, C., Addicks, K. & Hescheler, J. (1999) *FASEB J.* **13,** 313–324.
23. Hamill, O. P., Marty, A., Neher, E., Sakmann, B. & Sigworth, F. J. (1981) *Pflugers Arch.* **391,** 85–100.
24. Korn, S. J. & Horn, R. (1989) *J. Gen. Physiol.* **94,** 789–812.
25. Kimura, J., Noma, A. & Irisawa, H. (1986) *Nature (London)* **319,** 596–597.
26. Mechmann, S. & Pott, L. (1986) *Nature (London)* **319,** 597–599.
27. Barcenas-Ruiz, L., Beuckelmann, D. J. & Wier, W. G. (1987) *Science* **238,** 1720–1722.
28. Orchard, C. H., Eisner, D. A. & Allen, D. G. (1983) *Nature (London)* **304,** 735–738.
29. Saitoh, M., Oyamada, M., Oyamada, Y., Kaku, T. & Mori, M. (1997) *Carcinogenesis* **18,** 1319–1328.
30. Fishman, M. C. & Chien, K. R. (1997) *Development (Cambridge, U.K.)* **124,** 2099–2117.
31. Nayler, W. G. & Fassold, E. (1977) *Cardiovasc. Res.* **11,** 231–237.
32. Mahony, L. & Jones, L. R. (1986) *J. Biol. Chem.* **261,** 15257–15265.
33. Klitzner, T. S. & Friedman, W. F. (1989) *Pediatr. Res.* **26,** 98–101.
34. Chin, T. K., Friedman, W. F. & Klitzner, T. S. (1990) *Circ. Res.* **67,** 574–579.
35. Kolossov, E., Fleischmann, B. K., Liu, Q., Bloch, W., Viatchenko-Karpinski, S., Manzke, O., Ji, G. J., Bohlen, H., Addicks, K. & Hescheler J. (1998) *J. Cell Biol.* **143,** 2045–2056.
36. Clusin, W. T. (1983) *Nature (London)* **301,** 248–250.
37. Clusin, W. T., Fischmeister, R. & De Haan, R. L. (1983) *Am. J. Physiol.* **245,** H528–H532.
38. Lipp, P. & Pott, L. (1988) *J. Physiol. (London)* **403,** 355–366.
39. DiFrancesco, D. & Noble, D. (1985) *Philos. Trans. R. Soc. London Ser. B* **307,** 353–398.
40. Tsien, R. W., Kass, R. S. & Weingart, R. (1979) *J. Exp. Biol.* **81,** 205–215.
41. Kamino, K. (1991) *Physiol. Rev.* **71,** 53–91.
42. Bers, D. M. & MacLeod, K. T. (1986) *Circ. Res.* **58,** 769–782.
43. Hordof, A. J., Spotnitz, A., Mary Rabine, L., Edie, R. N. & Rosen, M. R. (1978) *Circulation* **57,** 223–229.
44. Kass, R. S., Tsien, R. W. & Weingart, R. (1978) *J. Physiol. (London)* **281,** 209–226.
45. Clusin, W. T., Bristow, M. R., Karagueuzian, H. S., Katzung, B. G. & Schroeder, J. S. (1982) *Am. J Cardiol.* **49,** 606–612.
46. Clusin, W. T., Buchbinder, M. & Harrison, D. C. (1983) *Lancet* **1,** 272–274.
47. Clusin, W. T. (1983) *Proc. Natl. Acad. Sci. USA* **80,** 3865–3869.
48. Kass, R. S., Lederer, W. J., Tsien, R. W. & Weingart, R. (1978) *J. Physiol. (London)* **281,** 187–208.